Plasma Chemistry and Plasma Processing, Vol. 22, No. 3, September 2002 (© 2002)

Comparative Calorimetric Study of ICP Generator with Forward-Vortex and Reverse-Vortex Stabilization

A. Gutsol,[1] J. Larjo,[2] and R. Hernberg[2]

Received April 4, 2000; accepted January 1, 2001

Different methods of ICP stabilization are discussed, including the Reverse Vortex Stabilization, for which no previous well-described implementation is in science literature. Comparative calorimetric study was performed for two methods of stabilization: the Forward Vortex and the Reverse Vortex ones. Experiments were made for the ICP torch of invariable geometry with the power supply plate power up to 50 kW. Experimental technique is described and the tables with experimental data are presented. The efficiency of two studied methods is discussed primarily from the standpoint of plasma jet generation. It is demonstrated that the reverse-vortex stabilization is more efficient for almost all possible applications of ICP.

KEY WORDS: ICP torch; RF plasma generator; plasma stabilization; reverse vortex; calorimetric investigation.

1. INTRODUCTION

Inductively Coupled Plasma (ICP) torches (or Radio Frequency (RF) plasma generators) first described by Reed[1,2] are widely applied, mainly for high temperature treatment of materials. Their advantages compared to arc plasma torches are the absence of electrodes, which ensures high purity of the plasma, rather low flow velocity, and large volume of the plasma. In comparison with Micro-Wave (MW) plasma generators ICP torches also have some advantages: the enthalpy of a RF inductive plasma is generally higher than that of a MW plasma and RF power supplies of various frequency and power are relatively simple and well available.

[1]Institute of Chemistry and Technology of Rare Elements and Mineral Raw Materials, Kola Science Center of the Russian Academy of Sciences, Fersman St., 14, Apatity, Murmansk Reg., 184200, Russia. E-mail: gutsol@chemy.kolasc.net.ru (Present address: University of Illinois at Chicago, Department of Mechanical Engineering (MC 251), 842 West Taylor Street, Chicago, Illinois 60607-7022, USA, E-mail: agutsol@uic.edu)
[2]Tampere University of Technology, Optics Laboratory, P.O. Box 692, FIN-33101 Tampere, Finland. E-mails: larjo@cc.tut.fi; hernberg@cc.tut.fi

0272-4324/02/0900-0351/0

ICP torches have good rotational symmetry and the low gas and plasma flow velocities ensure the absence of turbulence in the plasma volume (plasma fire-ball, plasmoid). In an atmospheric pressure ICP the Local Thermodynamic Equilibrium (LTE) condition is valid with a high accuracy, so ICP torches are popular targets for physical and numerical modeling. Unfortunately, the experimental study of local conditions in ICP, in particular velocity field measurement in the high temperature zone is very difficult. Therefore the results of the simulation are not always compared with the applicable experimental data.

The recently developed method of reverse-vortex stabilization and heat insulation[3] has been tested in MW plasma torch[3–5] and gas combustion chamber.[5,6] The obtained results show that technically simple transformation from traditional forward-vortex stabilization and heat insulation method to the reverse-vortex method significatly changes the flow patterns in the described devices and improves considerably their basic characteristics. So, it seemed very promising to apply the reverse-vortex stabilization techniques to an ICP generator.

In this paper the principle of reverse-vortex stabilization of electric discharges is described for the case of the ICP. The results of comparative experimental study of an argon ICP torch with both forward-vortex and reverse-vortex stabilizations are also presented.

2. METHODS OF ICP STABILIZATION

To explain the purpose and principle of the reverse-vortex stabilization (Fig. 1f) it is necessary to review other known methods of ICP stabilization (Fig. 1a–1e). To limit the article length, we shall not consider the material in a historical succession; rather we proceed from simple to complex stabilization methods treating the stabilization process from the modern point of view.

With no plasma gas flow (Fig. 1a) an inductively coupled RF discharge can be stabilized inside a cooled tube (1). In some cases it is enough to ensure natural air convective cooling of quartz or even of a glass tube.[7] The reason for the space stability of such a discharge and the thermal stability of a glass tube wall is the Ampere force caused by the interaction of the alternating current induced predominantly in the skin-layer (3) of the plasma (4) and the magnetic field of the inductor (2). The Ampere force acts primarily in the radial direction, towards the axis of the plasmoid (4) and results in the formation of plasma recirculation zones. So, the electromagnetic convective heat insulation and stabilization of inductively coupled plasma is a self-organized process. The role of electrodynamical convection was clearly shown for the first time in the papers.[8–10] It has also been experimentally

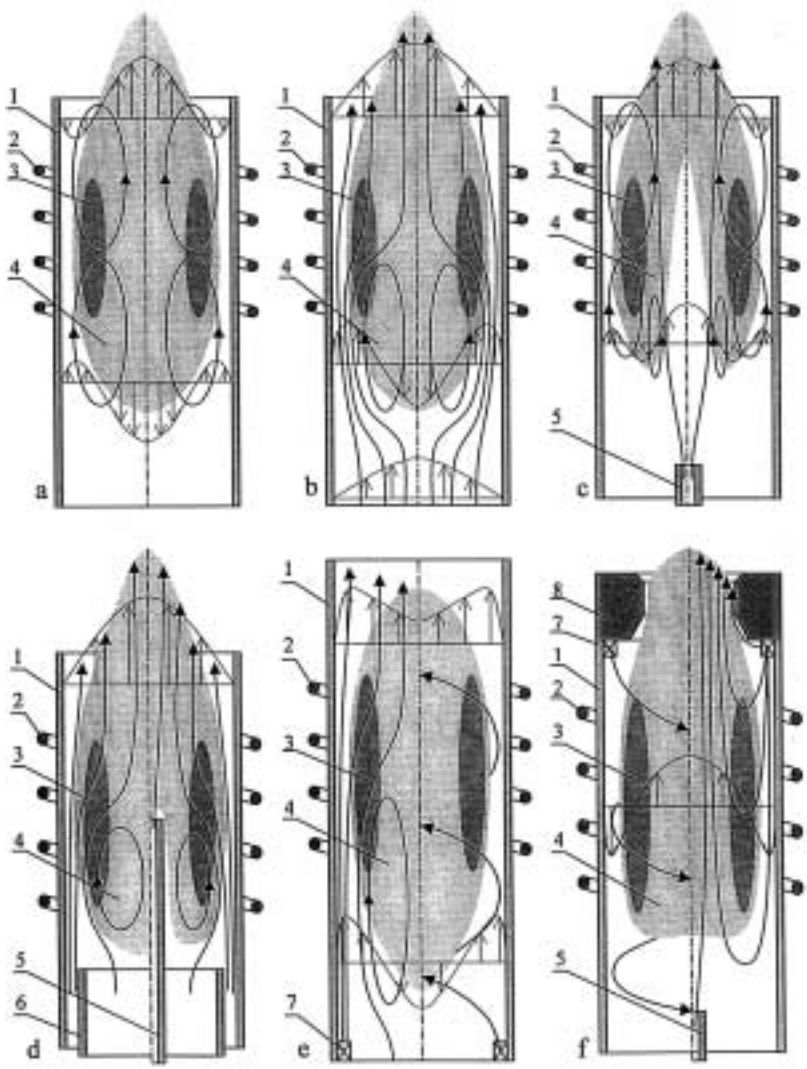

Fig. 1. Different schemes of ICP stabilization with streamlines (thick lines) and axial velocity profiles (thin lines): a, stabilization by electromagnetic forces only; b, stabilization in straight gas flow; c, stabilization by central high speed gas jet; d, stabilization inside the near-wall flow, with central cooling injection tube (right side); e, stabilization inside swirl flow—forward vortex stabilization; f, stabilization inside swirl flow—reverse vortex stabilization, with additional axial jet (right side). 1, quartz tube; 2, induction coil; 3, skin layer; 4, inductively coupled plasma; 5, central (probe) tube for axial injection of gas or treated material; 6, intermediate tube for near-wall stream formation; 7, tangential gas feeder for swirl flow formation; 8, water-cooled nozzle.

proved that pressure rises in an ICP as a result of electromagnetic contraction.[11]

If the heat transfer from the plasmoid to the walls is weak, i.e., if the plasmoid diameter is much smaller than the tube diameter, the plasmoid axial position is unstable.[7] If such a plasmoid is blown by plasma gas obeying a Poiseuille velocity profile (Fig. 1b), its stabilization is improved. The plasmoid stabilization inside plasma gas flow is probably analogous to ping-pong ball stabilization in a stream of air or water: side displacement from the axis results in a flow aceleration on the opposite side and an aerodynamic "lifting" force induces the back displacement. In the plasma, an increment of the gas flow leads to downstream shear of the plasmoid.[7,11] The further increment of the flow results in blowing out of the discharge. In this process the main role is played by the rather low speed of the quasi-equilibrium discharge propagation due to thermal conductivity, a process similar to flame front propagation. According to calculations,[12–14] the rate of the discharge propagation in cold argon is several centimeters per second. Therefore, the destruction of plasmoid recirculation zones (the speed of recirculation can reach several meters per second[10]) by the plasma gas flow (Fig. 1b) results in immediate blowing out of the discharge.

If an axial high-velocity narrow gas jet is directed at the plasmoid, it will improve the discharge stabilization, probably because of the formation of secondary recirculation zones (Fig. 1c). This method of stabilization was first proposed in the very first paper of Reed.[1] Despite the first impression, this method is not very convenient for disperse material injection to the plasma. The formed secondary eddies (Fig. 1c) will catch some material from the central jet and precipitate it on the tube (1) wall.[15] Besides, the high flow speed limits the particle residence time in the plasma.

The method of stabilization using a near-wall high-velocity axial gas stream (Fig. 1d) was also first described by Reed[2] and was widely applied. This method can be combined[2] with an additional flow through an inner tube (6), or be applied only by itself.[10] The near-wall stream has no effect on the upstream eddy of recirculation. In the coil region this stream partially penetrates into the plasma (4). The reasons for this penetration are the Ampere force and gas expansion because of heating from the plasma and stream stagnation due to the viscous friction. The additional flow through the inner tube (6) moves the plasmoid away from the tube, preventing the overheating of this tube. Naturally, the additional flow velocity should be low enough not to decay the upstream eddy of recirculation. This method of stabilization can be combined with the use of a high-velocity narrow axial stream (Fig. 1c) for dispersed material transportation, as in paper.[15] If stronger heating of the treated material is required, it is necessary to insert a cooled probe for material feeding downstream the recirculation zone

(sometimes up to the middle of the coil[16]), as shown in the right side of Fig. 1d. This allows disperse material feeding with low speed and no precipiation to the tube wall.

Swirl stabilization of the ICP, also first proposed by Reed,[1] is widely applied (Fig. 1e). To distinguish this method of stabilization from the reverse-vortex presented by us, this classical method (Fig. 1e) is called forward-vortex stabilization (FVS). This method is not very convenient for disperse material treatment, as the flow rotation can reject part of the particles from the plasma due to the centrifugal force. However, considering the actual stabilization and heat insulation this is probably one of the most effective methods. Reed[1] probably applied this method with understanding of the deep analogy between the processes of discharge and flame propagation. Rayzer[12–14] has subsequently developed this analogy. FVS is used in powerful ICP generators for gas heating in facilities for simulation of conditions of spacecraft re-entry[17] and also very widely in devices for gas incineration.[18] The intense flow rotation results in formation of a recirculation zone in the vicinity of the swirl feeder (7) (Fig. 1e). The length of this zone in cold gas may be as long as some tens of the tube diameter.[19] The reverse flow on the axis of the zone results in formation of a plasma "tail" far upstream of the inductor region.[12–14] In addition to the recirculation zone, which is usually necessary for discharge propagation when the electric field is weaker than required for gas electric breakdown,[20] the swirl flow generates a strong radial pressure gradient. This makes the high temperature plasmoid "float" to the axis because of the buoyancy force in the centrifugal field. Effect of buoyancy can be easily estimated by the ratio of the square of the Reynolds number (Re) to Grashof number (Gr), which is equal to the ratio of the inertial force to buoyant force. When this ratio is much smaller than unity, buoyancy effect is dominant. If a gas with density ρ, viscosity μ, and temperature coefficient of volumetric expansion β (for the ideal gases $\beta = 1/T$, where T is gas temperature), rotates inside the cylindrical tube of radius R with tangential velocity v and has contact with thermal plasma of temperature $T_p \sim 10{,}000\,\mathrm{K}$, then temperature difference $\Delta T = T_p - T \approx T_p$ and

$$\begin{aligned}(\mathrm{Re})^2/\mathrm{Gr} &= (\rho v R/\mu)^2/(\rho^2 g R^3 \beta \Delta T/\mu^2)\\ &= v^2(gR\beta\Delta T)^{-1}\\ &= v^2((v^2/R)R\beta\Delta T)^{-1}\\ &= (\beta\Delta T)^{-1}\\ &\approx 0.03\end{aligned}$$

(We took into account that in the case of strong rotation the centrifugal acceleration $g = v^2/R$ plays a role of gravity acceleration g_0. For the typical

conditions of swirl stabilization $g = (30 - 300)g_0$). So, buoyancy is the really dominant effect in the case of any kind of vortex stabilization. This effect of plasmoid "floating" is a reason of wide application of the vortex methods for heat insulation of plasma in different electric discharges.[21]

The reverse-vortex stabilization (RVS) method (Fig. 1f) presented in this paper was applied earlier in an MW discharge[3–5] and in a gaseous flame.[5,6] The basic idea of this method is to allow the reverse flow, formed near the swirl feeder (7), to leave the discharge volume without mixing with the incoming flow and with no recirculation zone formation. The water-cooled nozzle (8) near the swirl feeder (7) prevents the immediate exit of the rotating incoming gas from the torch. Before leaving the torch through the nozzle, the plasma gas should lose some of its angular momentum due to viscous friction with the tube wall. The principal differences between this method of stabilization and all the others are: first, all the plasma volume is vented by the plasma gas, i.e., there are no stagnant zones of recirculation; second, practically all plasma gas flows through the high temperature zone. These properties of the reverse-vortex method of stabilization are very promising for plasma chemical applications. The high temperature zone appears to be hydrodynamically separated from the walls irrespective of the Ampere force. The experiments with a MW discharge of 3.5 kW power and with a flame of 2 kW power have shown that such a technically simple modification of the vortex stabilization system reduces the power losses from the high temperature zone to the device walls by a factor of 5–7 and therefore simplifies considerably the requirements of the wall materials.[3–6] The low axial and radial gas velocities in the hot zone of the RVS plasma (Fig. 1f) are the basis of its stability considering the discharge propagation rate. Additional axial gas feed through the pipe (5) should not significantly transform the flow system, so the feed velocity can be varied in a wide range. It is not so clear how strongly the flow rotation will affect the treatment of disperse material injected with the additional axial flow. Radial migration of turbulent micro-volumes decelerated near the tube walls should form a central zone with low rotation velocity.[4,22] Some authors have made experiments with intense rotating flows and observed the formation of central zones with a low rotation velocity[23] or even reverse rotation.[24,25] Anyway, our test experiment with axial input of zirconium dioxide powder into MW discharge of 3.5 kW power with the RVS has demonstrted the spheroidization of particles with the size up to 100 microns,[3,4] that means passing of powder particles through the discharge zone.

Different stable forms of the RVS argon ICP were observed in 10–100 kPa pressure range in the preliminary experiments and were described in previous publications.[26,27] During this investigation we have found one rarely cited publication[28] by Reed and have seen that he also had used the

reverse-vortex stabilization of the ICP in one of his spectroscopic experiments. The plasma torch was submerged into water for cooling and Reed did not comment the applied method of stabilization in any way. So, it remains unclear whether he saw other advantages of this method, except for an opportunity to observe discharge radiation without any obstacles from the closed end of the torch. Anyway, this is an occasion to once again admire the talent of this scientist and to recall that old achievements may often be forgotten in the pursuit of new results. Nevertheless, we should emphasize that we do not know of any previous well-described implementations of RVS ICP.

3. CALORIMETRIC STUDY OF THE REVERSE-VORTEX AND FORWARD-VORTEX STABILIZED ICP GENERATORS

To compare the efficiencies of the RVS ICP and Forward-Vortex Stabilized (FVS) ICP torces of the same geometry as plasma jet generators, total calorimetric measurements were made using atmospheric pressure argon plasma. A scheme of measurements is presented in Fig. 2.

The plasma torch can operate in RVS or FVS configuration. The discharge volume (7) is confined by a quartz tube with inner diameter of 75 mm. A water-cooled inductive coil with inner diameter of 90 mm and length of 100 mm supplies the RF electromagnetic energy from RF generator (2) (the model ВЧИ 11-60/1,76, made in USSR). When the torch operated in FVS configuration argon flow from cylinders (4) measured by rotameters (3) entered the discharge volume (7) tangentially through the lower feeder (5) with six square openings (square side 2 mm) on the radius 38 mm. In this case the torch geometry differs from the FVS ICP torch usually used only by the nozzle ((8) on Fig. 1f) on the plasma exit end. We used a nozzle of 43 mm length and 25 mm smallest inner diameter. In the RVS case argon entered the quartz tube through the upper feeder of inner diameter of 72 mm that has four circular tangential inlets of 2 m diameter. The upper feeder and the nozzle were combined into the nozzle-feeder unit ((8) on Fig. 2). The quartz tube length was 380 mm and the center of the inductive coil was at 130 m from the feeder side of the nozzle.

After a preliminary study[26,27] the plasma torch scheme was modified for the calorimetric measurements to provide water-cooling of all surroundings. We also implemented water film cooling of the quartz tube (probably similar to that used by Boulos[29]), shown in Figs. 2 and 3. A stainless steel multi-tube heat exchanger ((9) on Fig. 2) of 50 cm length was mounted downstream of the plasma torch to measure the exhaust gas enthalpy. Measurement of the argon temperature after the heat exchanger indicated that heat loss after this point was negligible. The powers absorbed by the

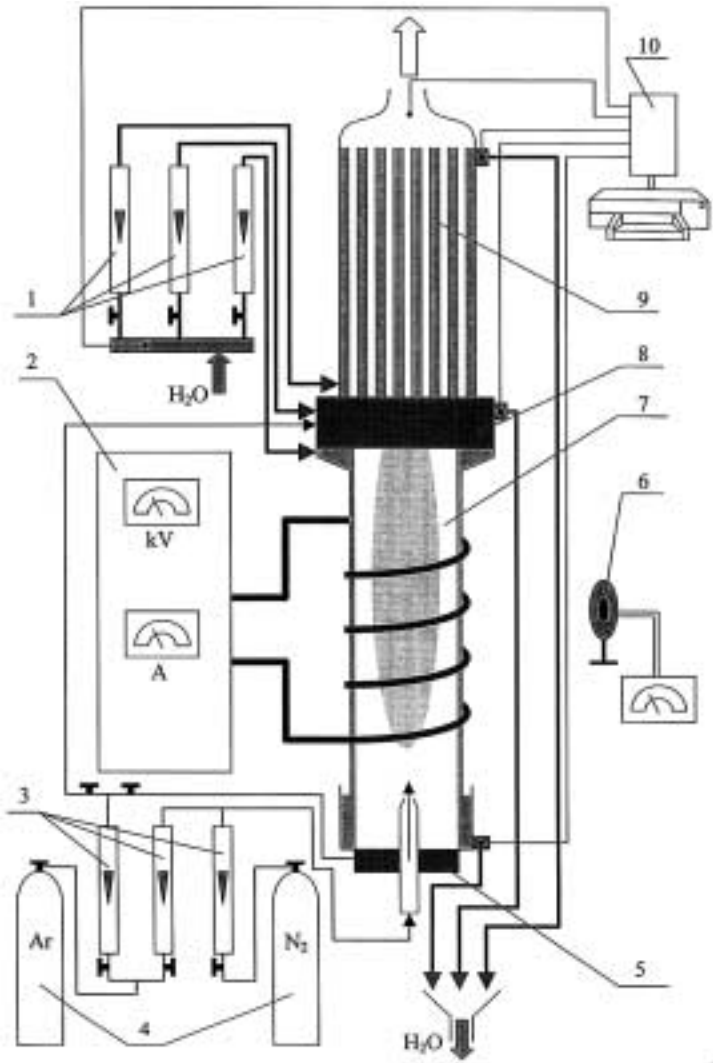

Fig. 2. Scheme of calorimetric measurements: 1, water flow meters; 2, RF generator; 3, gas flow meters; 4, cylinders with compressed gases; 5, the lower tangential gas flow feeder; 6, blackbody surface absorber with monitoring device; 7, ICP torch with water film surface cooling of the quartz tube; 8, the upper tangential gas flow feeder combined with the nozzle; 9, multi-tube heat exchanger; 10, multi-channels interface for thermocouples data acquisition with shielded K-type thermocouples and a printer.

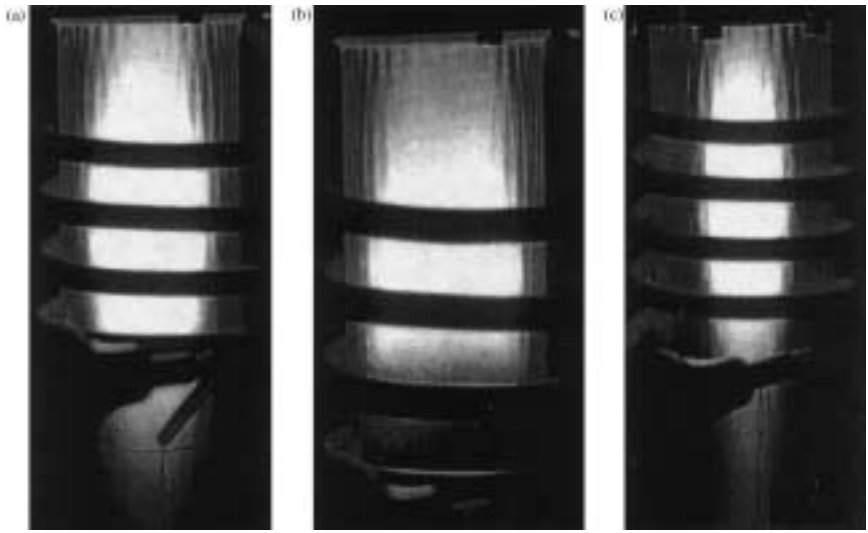

Fig. 3. Photographs of RF inductive discharges in the modified torch with different stabilization: (a) forward vortex stabilization, plate power: 16 kW, argon mass flow: 1.4 g/s; (b) reverse vortex stabilization, plate power; 16 kW, argon mass flow: 2.1 g/s; (c) reverse vortex stabilization, plate power; 16 kW, argon mass flow: 0.57 g/s.

heat exchanger $W_{h/e}$, nozzle W_n and the tube W_t were measured separately. For this aim we measured temperature and flow rate of cooling water flows. For flow rate measuring we used "KROHNE VA 20" rotameters (1). For temperature measuring we used K-type shielded thermocouples. For thermocouples data acquisition we used 16-channels interface (10) (model SR630, manufactured by Stanford Research Systems, Inc.). Data were read and printed every 12 s. The calorimetric system resolution was about 20 W. Obtained experimental data are presented in Tables I (FVS ICP) and II (RVS ICP).

We have also measured the total radiation intensity at about 1.3 m distance from the plasma with a blackbody surface absorber (6), which is usually used for laser radiation measuring. Then we calculated the total radiation loss W_r with account of partial blockage of radiation by the non-transparent inductor coil and absorption by water-cooled parts of the plasma torch (nozzle-feeder unit (8), heat exchanger (9) and quartz tube together with the lower feeder (5)). The accuracy of radiation measurements was about 7% and was much worse than accuracy of calorimetric measurements. The sum of all the measured losses (nozzle, tube, radiation, and heat exchanger) is equal to the total energy W_d initially absorbed by the plasma from the inductive coil: $W_d = W_n + W_t + W_r + W_{h/e}$. Estimations and testing

Table I. Experimental Data on Heat Losses for FVS ICP

No.	U [kV]	I [A]	W_{pp} [kW]	Q_{Ar} [g/s]	$W_{h/e}$ [kW]	W_n [kW]	W_t [kW]	W_r [kW]
1	2.0	2.0	4.0	1.40	1.09	0.23	0.71	0.24
2	2.5	2.5	6.25	1.40	1.76	0.40	0.97	0.60
3	3.0	3.0	9.00	1.40	2.35	0.65	1.30	1.07
4	3.5	3.5	12.25	1.40	2.88	0.95	1.79	1.87
5	4.0	4.0	16.00	1.40	3.38	1.38	2.99	2.68
6	4.0	4.0	16.00	1.40	3.36	1.30	2.61	2.94
7	5.0	5.0	25.00	1.40	4.13	1.57	4.47	5.89
8	5.0	5.0	25.00	2.29	5.81	1.46	3.48	6.29
9	5.0	5.0	25.00	3.21	7.14	1.01	3.05	5.89
10	6.0	6.0	36.00	1.40	4.09	1.81	8.82	7.63
11	7.0	7.0	49.00	1.40	4.20	2.12	13.65	11.78

experiments showed that the total discharge power W_d was measured with about 3% accuracy. This power was 55–75% of the plate power W_{pp} of the RF generator depending on the discharge regime and stabilization method. The plate power of the RF generator was calculated by multiplying the anode voltage U and anode current I. The accuracy of plate power measuring was poorer because of the low resolution of the monitoring devices. The reproducibility of the discharge regime was not very high either, as the final adjusting of the generator-discharge system could be made only after the discharge ignition. The reproducibility problem results in redistribution of energy into different losses channels (see, for example, data for experiments 5 and 6, Table I), but total discarge energy W_d and plasma jet energy (equal to $W_{h/e}$) were relatively insensitive to this problem.

4. DISCUSSION

Obtained experimental data (Tables I and II) may be analyzed by different ways. So, the experiments with a FVS ICP (Table I) in the geometry with the contracted plasma exit (with the nozzle) have shown the extremely high stability of this discharge. It is possible to change the RF generator power by an order of magnitude with the same argon mass flow, and the discharge (Fig. 3a) remains stable (Fig. 4), only its brightness and volume change and relative energy losses into different channels (Fig. 5) change also. The power characteristics of the FVS ICP, such as the dependence of the average plasma jet enthalpy $H_p = (W_j/Q_{Ar})$ on the plate power (Fig. 6) and the dependence of the plasma torch efficiency on the discharge power (Fig. 7) are typical. Here the plasma torch efficiency η is the ratio of the plasma jet power W_j (we assume that W_j is equal to the power absorbed by

Table II. Experimental Data on Heat Losses for RVS ICP

No.	U [kV]	I [A]	W_{pp} [kW]	Q_{Ar} [g/s]	$W_{h/e}$ [kW]	W_n [kW]	W_t [kW]	W_r [kW]
1	3.5	3.5	12.25	1.01	2.39	1.26	2.18	1.88
2	3.5	3.5	12.25	1.12	2.65	1.32	2.18	2.03
3	4.0	4.0	16.00	0.42	1.37	1.20	4.91	2.75
4	4.0	4.0	16.00	0.57	1.91	1.19	5.12	3.51
5	4.0	4.0	16.00	1.40	3.48	1.39	2.50	2.01
6	4.0	4.0	16.00	1.79	4.49	1.43	2.23	1.48
7	4.0	4.0	16.00	2.08	4.36	1.53	2.18	1.34
8	4.0	4.0	16.00	2.08	5.55	1.44	2.10	1.00
9	4.0	4.0	16.00	2.29	5.89	1.52	2.10	1.07
10	4.5	4.5	20.25	2.47	6.87	1.66	2.60	1.74
11	5.0	5.0	25.00	1.40	3.63	1.51	5.73	4.06
12	5.0	5.0	25.00	2.08	5.79	1.93	4.43	2.63
13	5.0	5.0	25.00	2.29	6.57	1.85	3.89	2.14
14	5.0	5.0	25.00	3.21	9.24	2.16	2.79	1.74
15	5.0	5.0	25.00	3.21	9.07	2.06	2.86	2.01
16	6.0	6.0	36.00	1.40	3.67	1.68	9.89	7.07
17	6.0	6.0	36.00	2.08	5.79	2.07	8.52	5.67
18	6.0	6.0	36.00	2.29	6.72	2.10	8.00	5.45
19	6.0	6.0	36.00	3.21	9.97	2.37	5.25	3.51
20	6.0	6.0	36.00	3.21	9.91	2.25	5.12	3.75
21	7.0	7.0	49.00	1.40	3.68	1.89	14.83	12.06
22	7.0	7.0	49.00	2.08	5.90	2.37	13.52	10.04
23	7.0	7.0	49.00	2.29	6.78	2.33	12.50	9.82
24	7.0	7.0	49.00	3.21	10.03	2.58	10.09	8.37
25	7.0	7.0	49.00	3.21	10.15	2.48	10.08	8.58
26	5.0	5.0	25.00	2.29 + 1.40 axial	6.98	1.35	3.68	2.01
27	7.0	7.0	49.00	2.29 + 0.85 N_2 axial	17.66	3.02	9.22	6.57

the heat exchanger $W_{h/e}$) to the total discharge power W_d: $\eta = W_j / W_d$. Plate power increase under a constant argon mass flow rate results in an increase of the average plasma jet enthalpy, up to the enthalpy level of 3 kJ/g. Argon mass flow rate increase under a constant plate power results in a decrease of the average plasma jet enthalpy (Fig. 6). The plasma torch efficiency drops with the growth of the discharge power and with the decrease of argon mass flow rate (Fig. 7). Thus, the FVS ICP is able to generate a high enthalpy plasma jet with low efficiency or a low enthalpy plasma jet with rather high efficiency.

The plasma torch efficiency for the RVS (Fig. 8) also drops with the growth of the discharge power and the decrease of the gas flow rate, though η reaches a higher level than in the FVS ICP. The average enthalpy of the

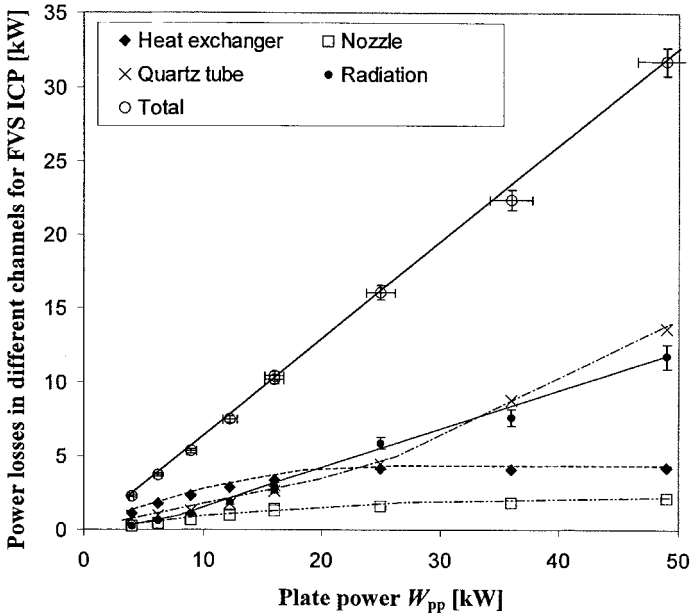

Fig. 4. Argon FVS ICP. Dependence of the power losses in different channels and the total discharge power W_d on the RF generator plate power W_{pp}.

argon plasma jet generated by the RVS ICP is higher than 2 kJ/g in all cases. It does not grow only with the plate power, but also with the argon mass flow rate (Fig. 9), which is extremely unusual for any type of discharge. It is possible to understand the reason for this phenomenon from the result of the numerical simulation[30] and flow pattern on Fig. 1f. The gas flows mostly through the active discharge zone and after that its enthalpy rises to a very high and approximately constant level. When gas flow is low an additional recirculation zone is formed in the closed part of the discharge tube due to the Ampere force. This recirculation zone is similar to the zones presented in Fig. 1(a–e), which are also formed due to the Ampere force. This recirculation creates the plasma "tail," observed in some conditions during the preliminary study,[26,27] and results in some additional heat and radiation losses. (In Fig. 5 and Table II it is possible to see that the fraction of the radiation losses in the total energy balance of the RVS ICP torch varied in a wide range: from 8 to 32%.) The increase of the plasma gas flow results in shrinking of the additional recirculation zone and the plasma volume (see Fig. 3b). This leads to a significant reduction of heat losses via the quartz tube and radiation, so the average plasma jet enthalpy increases.

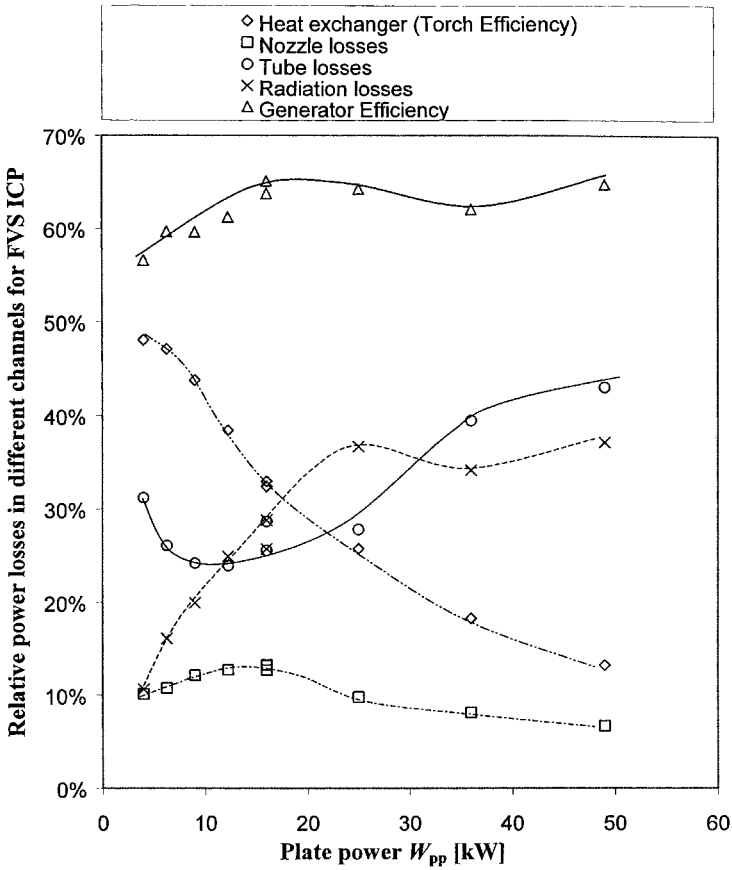

Fig. 5. Argon FVS ICP. Dependence of the relative power losses in different channels (tube, W_t/W_d; nozzle, W_n/W_d; radiation, W_r/W_d), plasma torch efficiency ($\eta = W_j/W_d = W_{h/e}/W_d$), and the generator efficiency (generator—plasma torch coupling efficiency, W_d/W_{pp}) on the RF generator plate power W_{pp}.

This phenomenon indicates that the RVS ICP torch is capable of generating a high enthalpy plasma jet with a high efficiency. This property is very useful in various applications.

For a constant plate power the increase of the plasma jet generation efficiency with plasma gas flow growth for the RVS ICP torch is steeper than that for the FVS ICP (Fig. 10). For any constant plate power the highest efficiency was observed under the highest gas flow in the range of discharge stability. In this regime the discharge volume was so small that the plasma does not extend to the last inductor loop (Fig. 3b).

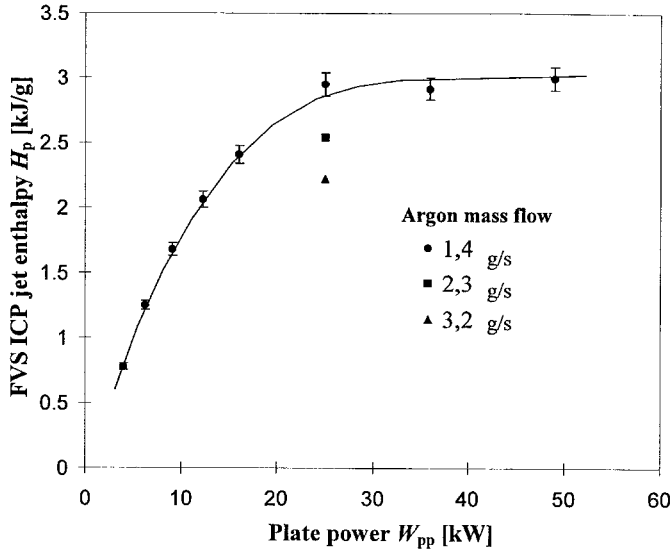

Fig. 6. Argon FVS ICP. Dependence of the average plasma jet enthalpy H_p on the RF generator plate power W_{pp} and argon mass flow Q_{Ar}.

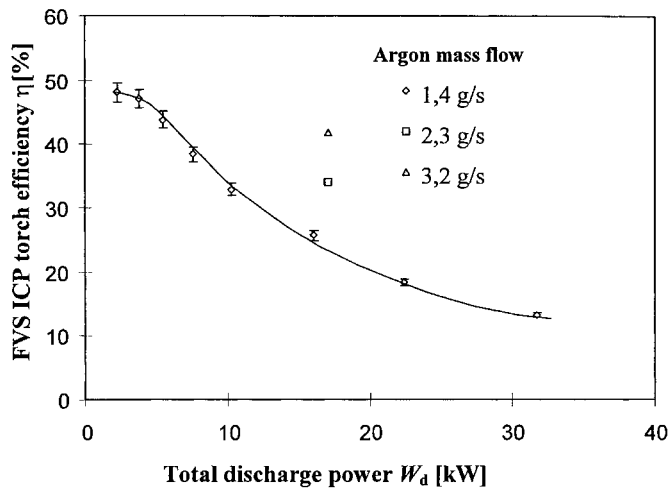

Fig. 7. Argon FVS ICP. Dependence of the plasma torch efficiency η on the total discharge power W_d and argon mass flow Q_{Ar}.

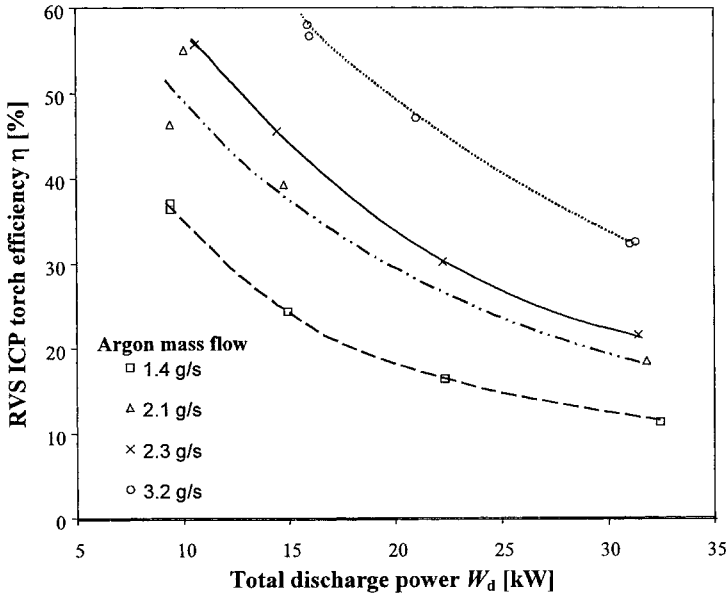

Fig. 8. Argon RVS ICP. Dependence of the plasma torch efficiency η on the total discharge power W_d for different argon mass flow Q_{Ar}.

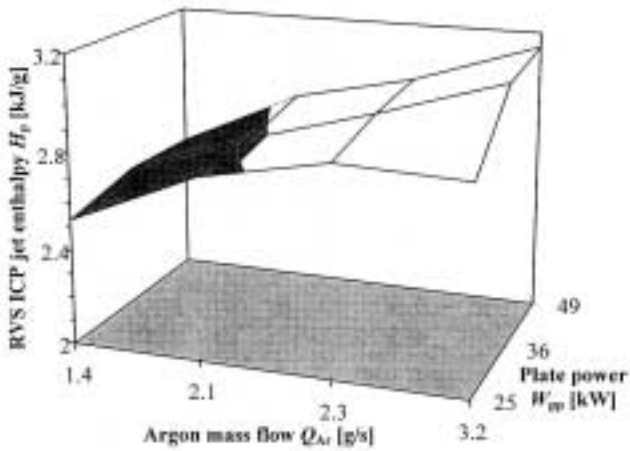

Fig. 9. Argon FVS ICP. Dependence of the average plasma jet enthalpy H_p on the RF generator plate power W_{pp} and argon mass flow Q_{Ar}.

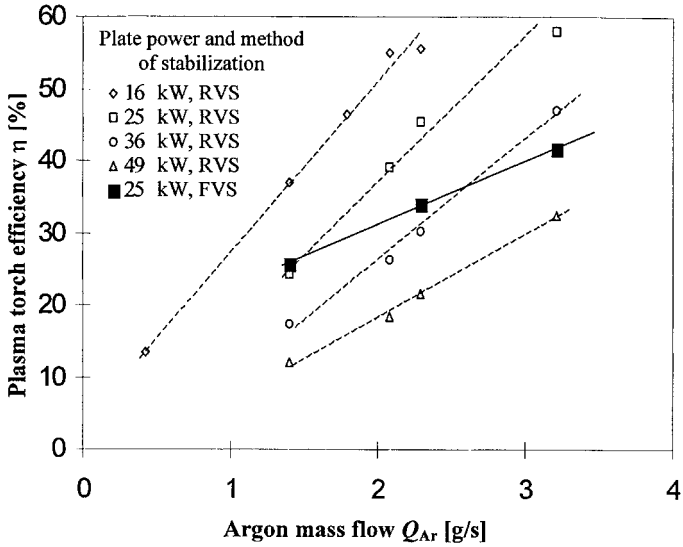

Fig. 10. Comparison of the plasma torch efficiency of FVS and RVS argon ICP. Dependence of the plasma torch efficiency η on the argon mass flow Q_{Ar} for different plate power.

Comparing the obtained plasma jet generation efficiency (up to 48% for the FVS and 58% for the RVS) of the studied argon RF plasma torches with a water-cooled nozzle with reliable data for other argon ICP torches (about 55% for the torch without a nozzle but with a water-cooled probe for material feeding;[31] up to 45% in Reed paper;[1] up to 37% in the papers cited in the article[32]), it becomes clear that the plasma jet generation efficiency of this RVS ICP torch is rather high. This is a promising property for those torches where the nozzle is a necessary design part, for example, in the sources of supersonic plasma jets.[33]

An efficiency of the studied discharges as high enthalpy plasma generators is presented in Fig. 11. Also in this figure data is presented for the lowest feasible gas consumption regime of this RVS ICP (about 0.5 g/s of argon under 16 kW plate power). In this case the active discharge zone is narrow and confined close to the plasma torch axis (Fig. 3c). In spite of the quite low efficiency (about 15%), this regime may be very suitable for some applications like spectral chemical analysis, where low pure argon consumption is very important. Considering the small argon mass flow and the relatively small plasmoid diameter, this discharge resembles the discharge described by Dymshits and Koretskiy.[7] However, the large length of plasmoid in the present case indicates some essential influence of gas dynamics, contrary to the situation described in the reference.

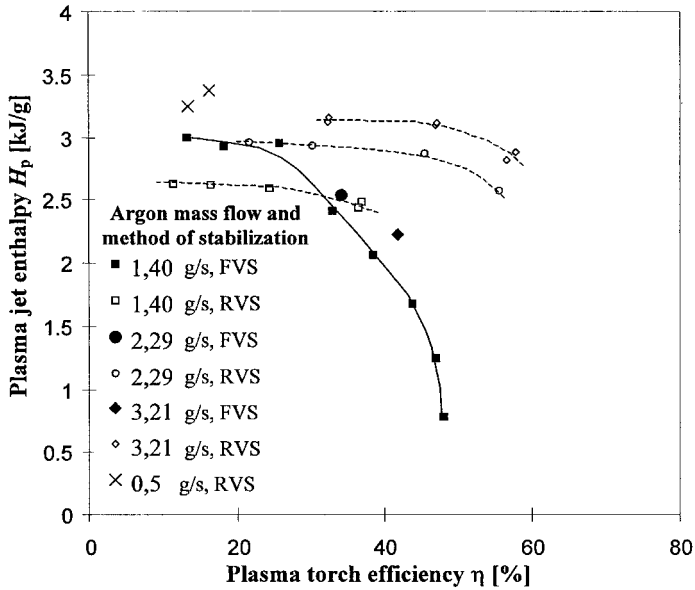

Fig. 11. Comparison of the efficiency of FVS and RVS argon ICP as high enthalpy plasma generators. Interrelation of the average plasma jet enthalpy H_p and plasma torch efficiency η for different argon mass flow Q_{Ar} and method of stabilization.

From the application point of view, probably the most promising property of the reverse vortex flows is the possibility of disrupting the flow pattern (Fig. 1f). Our experiments showed that the axial argon flow could be as strong as the main swirl argon flow without extinguishing the discharge. The calorimetric measurements of two similar regimes are also presented at the end of Table II. For example, consideration of the last one gives the next results: at 49 kW plate power, 2.29 g/s argon mass flow through the tangential feeder and additional 0.85 g/s of nitrogen mass flow through the axial tube, the discharge absorbed 36.46 kW (74.4% of plate power). With 48.4% efficiency, it generates a plasma jet with average enthalpy of 5.62 kJ/g. This corresponds approximately to temperature of 6000 K for the given mixture of an argon and nitrogen. Comparison of the results for the experiments with RVS 13 and 26, 23 and 27 (Table II) shows that really additional axial flow does not disrupt flow pattern substantially, as plasma torch efficiency $\eta = W_j/W_d$ increases with additional flow. Therefore, it may be possible to insert large quantities of material (gaseous or disperse) into plasma treatment in the active zone. According to our insight the treated products should not interact with the plasma torch wall significantly. This

property may open new opportunities in plasma technology, as the lack of such properties in traditional RF discharges restricts their applications in plasma chemistry.[34]

Thus, it is possible to conclude that RVS ICP torches are very promising for various applications and may find wider application than the traditional ICP torches.

This work was supported by The Academy of Finland and The Russian Foundation for Basic Research (Project 98-01-00021).

REFERENCES

1. T. B. Reed, *J. Appl. Phys.* **32**, 821 (1961).
2. T. B. Reed, *J. Appl. Phys.* **32**, 2534 (1961).
3. V. T. Kalinnikov and A. F. Gutsol, *Doklady Akademii Nauk* **353**, 469 (1997) (in Russian) [*Physics—Doklady* **42**(4), 179 (1997)].
4. A. F. Gutsol and J. A. Bakken, *J. Phys. D: Appl. Phys.* **31**, 704 (1998).
5. V. T. Kalinnikov and A. F. Gutsol, *Teplofizika vysokikh temperatur* **37**, 194 (1999) (in Russian) [*High Temp.* **37**, 172 (1999)].
6. V. T. Kalinnikov and A. F. Gutsol, *Doklady Akademii Nauk* **360**, 49 (1998) (in Russian) [*Physics—Doklady* **43**(5), 302 (1998)].
7. M. Dymshits and Ya. P. Koretskii, *Zhurnal Tekhnicheskoy Fiziki* [*Sov. Phys. Tech. Phys.*] **34**, 1677 (1964) (in Russian).
8. M. Dymshits and Ya. P. Koretskiy, *Zhurnal Tekhnicheskoy Fiziki* **39**, 1039 (1969) (in Russian) [*Sov. Phys. Tech. Phys.* **14**, 779 (1969)].
9. D.Chase, *J. Appl. Phys.* **40**, 318 (1969).
10. D.Chase, *J. Appl. Phys.* **42**, 4870 (1971).
11. S. V. Dresvin and Kh. El-Mikati, *Teplofizika vysokikh temperatur* [*High Temp.*] **15**, 1158 (1977) (in Russian).
12. Yu. P. Rayzer, *Zhurnal Prikladnoy Mekhaniki i Tekhnicheskoy Fiziki* [*J. Appl. Mech. Techn. Phys.*] (1968), No. 3, 3 (in Russian).
13. Yu P. Rayzer, *Uspekhi Fizicheskikh Nauk* [*Sov. Phys. Uspekhi*] **99**, 687 (1969) (in Russian).
14. Yu. P. Rayzer, *Lazernaya iskra i rasprostranenie razryadov* [*Laser spark and discharge propagation*], Nauka, Moscow (1974) (in Russian).
15. V. Donskoy, S. V. Dresvin, K. K. Voronin, and F. K. Volynets, *Teplofizika vysokikh temperatur* [*High Temp.*] **3**, 627 (1965) (in Russian).
16. Xi Chen and E. Pfender, *Plasma Chem. Plasma Proc.* **11**(1), 103 (1991).
17. N. Gordeev, I. S. Pershin, and M. I. Yakushin, Proceedings of the Third International Symposium on Environmental Testing for Space Programmes (ESTEC, The Netherlands, June 1997): SP-408, August 1997, p. 189.
18. N. Syred and J. M. Beer, *Combustion and Flame* **23**, 143 (1974).
19. A. Khalatov, *Teoriya i Praktika Zakruchennykh Potokov* [*Theory and Practice of Rotational Flows*], Naukova Dumka, Kiev (1989) (in Russian).
20. V. M. Batenin, I. I. Klimovskiy, G. V. Lysov, and V. N. Troitskiy, *SVCh-Generatory Plasmy: Fizika, Tekhnika, Primenenie* [*MW-Generators of Plasma: Physics, Techniques, Application*], Energoatomizdat, Moscow (1988) (in Russian).
21. *Vikhrevaya Termoizolyatsiya Plasmy* [*Vortex Heat Insulation of Plasma*] M. A. Gol'dshtik, ed., Institute of Thermophysics, Novosibirsk (1979) (in Russian).

22. A. F. Gutsol, *Uspekhy Fizicheskikh Nauk* **167**, 665 (1997) (in Russian) [*Russian Physics—Uspekhi* **40**, 639 (1997)].
23. G. N. Abramovich and R. S. Trofimov, *Inzhenerno-Fizicheskiy Zhurnal* **53**, 751 (1987) (in Russian).
24. V. E. Fin'ko, *Zhurnal Tekhnicheskoy Fiziki* **53**, 1770 (1983) (in Russian) [*Sov. Phys. Tech. Phys.* **28**, 1089 (1983)].
25. A. I. Kotelnikov, Private communication (1999).
26. A. Gutsol, J. Larjo, and R. Hernberg, 2nd International Symposium on Heat and Mass Transfer under Plasma Conditions (April 1999, Turkey), p. 129.
27. A. Gutsol, J. Larjo, and R. Hernberg, 14th International Symposium on Plasma Chemistry (August 1999, Prague), p. 227.
28. T. B. Reed, *J. Appl. Phys.* **34**, 3146 (1963).
29. M. I. Boulos and K. Chen, Proceedings of the 11th International Symposium on Plasma Chemistry (August 1993, England), Vol. 1, p. 263.
30. A. Gutsol, J. Larjo, and R. Hernberg, *Teplofiizika vysokikh temperatur* **39**, 187 (2001) (in Russian) [*High Temp.*] **39**, 169 (2001)].
31. A. Merkhouf and M. I. Boulos, 14th International Symposium on Plasma Chemistry (August 1999, Prague), p. 421.
32. V. Kh. Goykhman and V. M. Gol'dfarb, *Plasmokhimicheskie Reaktsii i Protessy* [*Plasma Chem. React. Proc.*], Nauka, Moscow (1977), p. 231 (in Russian).
33. M. Hollenstein, M. Rahmane, and M. I. Boulos, 14th International Symposium on Plasma Chemistry (August 1999, Prague), p. 257.
34. J. W. McKelliget and N. El-Kaddah, *J. Appl. Phys.* **64**, 2948 (1988).